NASA TECHNICAL NOTE

NASA TN D-4028

TWO DIFFERENT INTERPRETATIONS OF MEASURED DISSOCIATION-RATE CONSTANTS AND THEIR EFFECTS ON COUPLED VIBRATIONAL-DISSOCIATIONAL FLOWS OF OXYGEN OVER A WEDGE

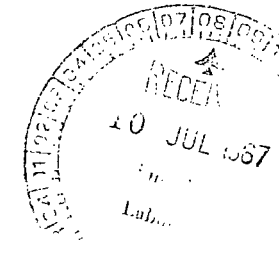

by Fred R. DeJarnette

Langley Research Center
Langley Station, Hampton, Va.

NATIONAL AERONAUTICS AND SPACE ADMINISTRATION • WASHINGTON, D. C. • JULY 1967

TWO DIFFERENT INTERPRETATIONS OF MEASURED DISSOCIATION-RATE CONSTANTS AND THEIR EFFECTS ON COUPLED VIBRATIONAL-DISSOCIATIONAL FLOWS OF OXYGEN OVER A WEDGE

By Fred R. DeJarnette

Langley Research Center
Langley Station, Hampton, Va.

NATIONAL AERONAUTICS AND SPACE ADMINISTRATION

For sale by the Clearinghouse for Federal Scientific and Technical Information
Springfield, Virginia 22151 – CFSTI price $3.00

TWO DIFFERENT INTERPRETATIONS OF MEASURED DISSOCIATION-RATE CONSTANTS AND THEIR EFFECTS ON COUPLED VIBRATIONAL-DISSOCIATIONAL FLOWS OF OXYGEN OVER A WEDGE

By Fred R. DeJarnette
Langley Research Center

SUMMARY

The coupling between vibrational nonequilibrium and dissociation has been shown previously to have a large effect on flow-field properties when dissociation is significant. However, most of the flow-field analyses presented to date used measured dissociation-rate constants in which the vibrational energy was assumed to be in equilibrium where the measurements were performed. Treanor has shown that this is not the case and that appreciable errors may result from the assumption of vibrational equilibrium in the measurements of dissociation-rate constants.

To illustrate the effects of vibrational relaxation on the measurements of dissociation-rate constants, this report presents computed flow-field properties for the nonequilibrium flow of oxygen over a wedge using both the coupled vibration-dissociation and the coupled vibration-dissociation-vibration models for two "limiting" conditions. One condition or interpretation assumes vibrational equilibrium in the rate constant measurements, whereas the other assumes that the rate constant measurements already include the vibrational nonequilibrium effects. The results showed significant differences between the flow-field properties for these two limiting conditions at a Mach number of 27.17 (where dissociation is appreciable) but small differences at a Mach number of 9.45 (where dissociation is small).

INTRODUCTION

The current emphasis on space travel has created an ever increasing demand for more accurate computations of the flow field surrounding reentry vehicles traveling at altitudes and velocities where real gas effects are important. In the most general sense "real-gas effects" means the consideration of finite rate gas chemistry and the effect of coupling between the various energy modes on these rates. Even at moderate hypersonic speeds, where dissociation is significant but ionization negligible, it has been shown that

the coupling of vibrational nonequilibrium and dissociation is important (refs. 1 and 2) even though the coupling mechanism itself is not very precisely understood.

A number of methods have been suggested for calculating the effect on reaction rates of interactions between the vibrational energy states and dissociation. Hammerling, Teare, and Kivel (ref. 1) developed a coupled vibration-dissociation (CVD) model which accounts for the vibrational nonequilibrium effects on the rate of dissociation. This CVD model was modified by Treanor and Marrone (ref. 2) to account for the dissociation nonequilibrium effects on the vibrational energy as well as the effect of vibrational nonequilibrium on dissociation (CVDV model). Reference 3 presents computed results for the nonequilibrium flow of nitrogen over a wedge, where the CVD and CVDV models are compared with the uncoupled model. Additional refinements to the CVDV model have been suggested by references 4, 5, and 6; however, their application to flows other than one-dimensional problems is quite tedious.

In most of the applications to date of the CVD and CVDV gas models, the computations were performed by assuming that the dissociation-rate constants were experimentally measured in a region where the vibrational energy was in equilibrium with the translational mode. Even the experimental investigators of references 7, 8, and 9 assumed that the vibrational energy was in equilibrium at the position aft of the shock wave where dissociation-rate constants were measured. However, Treanor, in a more recent report (ref. 10), indicates that the vibrational energy was not in equilibrium where the measurements were taken and that appreciable errors may result from the assumption of vibrational equilibrium. Also, Wray (ref. 11) found experimental evidence of the effect of vibrational relaxation on dissociation rates.

This report presents the inviscid flow-field properties for the nonequilibrium flow of oxygen over a wedge using both the CVD and CVDV coupling models. In order to assess the importance of the vibrational relaxation effects on measurements of dissociation-rate constants, flow-field properties are computed for two different interpretations of the rate constant measurements, referred to as "limiting" conditions herein. One condition considers the rate constant measured with vibrational equilibrium (as assumed by other investigators), whereas the other condition assumes that the measured rate constant already includes the nonequilibrium vibrational effects. For any given coupling model, calculations using rates determined in any other fashion should lie between these two limiting conditions. It should be noted, however, that the two limiting conditions used here may not be proper bounds for all types of flow fields.

SYMBOLS

a_m, b_m, d_m vectors used in equation (18) that correspond to terms in equations (1) to (5)

$E(T, T_v)$ term defined by equation (10)

E_v vibrational energy per unit mass

$\overline{E}_v = E_v / \overline{R} T_\infty$

f coupling factor defined by equation (17)

G(T) term defined by equation (11)

H enthalpy per unit mass

h Planck constant

k_f forward reaction-rate constant, $\frac{\text{centimeter}^3}{\text{mole-second}}$

k_r reverse reaction-rate constant, $\frac{\text{centimeter}^6}{\text{mole}^2\text{-second}}$

k_B Boltzmann constant

K_e equilibrium constant

m mass of an oxygen atom

M undisturbed free-stream Mach number

n,k number of increments in mesh system

N number of vibrational energy levels included in dissociation energy

$[O_2]$ concentration of O_2, mole/centimeter^3

p pressure, atmospheres (1 atmosphere = 101.3 kilonewtons per meter^2)

Q_O, Q_{O_2} electronic partition functions for O and O_2

$\bar{R}$ gas constant for O_2, $\bar{R} = R/W$

R universal gas constant

t time, seconds

T translational temperature, ^oK

$\bar{T} = T/T_\infty$

T_m temperature defined by equation (12), ^oK

T_v vibrational temperature, ^oK

u,v velocity components parallel and normal to the wedge surface, respectively

W molecular weight of O_2

x,y coordinates along and normal to wedge surface

α atom mass fraction

θ wedge half-angle

$\Theta_d, \Theta_R, \Theta_v$ characteristic dissociation, rotational, and vibrational temperatures, respectively, ^oK

ρ mass density

τ vibrational relaxation time, seconds

Subscripts:

e local equilibrium conditions

f forward reaction

meas measured

r reverse reaction

vib eq vibrational equilibrium

∞ undisturbed free-stream condition

Abbreviations:

CVD coupled vibration-dissociation model of reference 1

CVDV coupled vibration-dissociation-vibration model of reference 2

ANALYSIS

The gas model used here is a diatomic gas subject to harmonic vibrations, dissociation, and recombination. Translation and molecular rotation modes are assumed to be fully excited, whereas the electronic internal energy and ionization are neglected. Since the gas model used for the wedge flows herein is patterned after that used for the normal shock wave computations in reference 2, the same dissociation reactions and vibrational and dissociational rates as used in reference 2 are used here. For more detail concerning the gas model, see references 1, 2, 3, 12, and 13.

Figure 1 illustrates the flow geometry and body-oriented coordinate system for a wedge. The basic flow and rate equations for the steady, inviscid flow over a wedge are written in conservation form as (ref. 13):

Continuity:

$$\frac{\partial(\rho u)}{\partial x} + \frac{\partial(\rho v)}{\partial y} = 0 \tag{1}$$

x-momentum:

$$\frac{\partial(p + \rho u^2)}{\partial x} + \frac{\partial(\rho uv)}{\partial y} = 0 \tag{2}$$

y-momentum:

$$\frac{\partial(\rho uv)}{\partial x} + \frac{\partial(p + \rho v^2)}{\partial y} = 0 \tag{3}$$

Vibrational energy rate:

$$\frac{\partial(\rho u E_v)}{\partial x} + \frac{\partial(\rho v E_v)}{\partial y} = \rho \frac{dE_v}{dt} \tag{4}$$

Rate of dissociation:

$$\frac{\partial(\rho u \alpha)}{\partial x} + \frac{\partial(\rho v \alpha)}{\partial y} = \rho \frac{d\alpha}{dt} \tag{5}$$

Energy:

$$H + \frac{u^2 + v^2}{2} = \text{Constant} \tag{6}$$

The enthalpy and equation of state are

$$H = \left(\frac{7 + 3\alpha}{2}\right)\bar{R}T + (1 - \alpha)E_v + \alpha\bar{R}\Theta_d \tag{7}$$

$$p = \rho\bar{R}T(1 + \alpha) \tag{8}$$

For oxygen the vibrational rate is given by the CVDV model of Treanor and Marrone (ref. 2) as

$$\frac{dE_v}{dt} = \frac{E_{v,e} - E_v}{\tau} - \left[E(T,T_v) - E_v\right]\frac{1}{[O_2]}\left(\frac{d[O_2]}{dt}\right)_f + \left[G(T) - E_v\right]\frac{1}{[O_2]}\left(\frac{d[O_2]}{dt}\right)_r \tag{9}$$

where

$$E(T,T_v) = \bar{R}\Theta_v\left[\frac{1}{\exp(\Theta_v/T_m) - 1} - \frac{N}{\exp(N\Theta_v/T_m) - 1}\right] \tag{10}$$

$$G(T) = \bar{R}\Theta_v\left(\frac{N - 1}{2}\right) \tag{11}$$

$$\frac{1}{T_m} = \frac{1}{T_v} - \frac{1}{T} \tag{12}$$

For oxygen,

$$\tau p = 1.6 \times 10^{-9} \exp\left(\frac{101.44}{T^{1/3}}\right) \text{ atm-sec}$$

$$N = 26$$

$$\Theta_v = 2274^{\circ} \text{ K}$$

$$\Theta_d = 59\,380^{\circ} \text{ K}$$

with the use of a linear harmonic oscillator, E_v and $E_{v,e}$ can be written as (ref. 1):

$$E_v = \frac{\bar{R}\Theta_v}{e^{\Theta_v/T_v} - 1} \quad \text{and} \quad E_{v,e} = \frac{\bar{R}\Theta_v}{e^{\Theta_v/T} - 1}$$

The vibrational energy rate for the CVD model is given by the simpler expression

$$\frac{dE_v}{dt} = \frac{E_{v,e} - E_v}{\tau} \tag{13}$$

The following reactions, which are also the reactions used in reference 2, are used for the dissociation of oxygen:

$$O_2 + X \underset{k_r}{\overset{k_f}{\rightleftarrows}} 2O + X \qquad X = O, O_2$$

Therefore,

$$\frac{1}{[O_2]}\left(\frac{d[O_2]}{dt}\right)_f = k_f \frac{\rho(1+\alpha)}{W}$$

$$\frac{1}{[O_2]}\left(\frac{d[O_2]}{dt}\right)_r = k_r \frac{4\rho^2\alpha^2(1+\alpha)}{W^2(1-\alpha)}$$

and the net dissociation rate for oxygen is

$$\frac{d\alpha}{dt} = k_f \frac{\rho(1+\alpha)}{W}\left[(1-\alpha) - \frac{4\rho\alpha^2}{W}\frac{k_r}{k_f}\right] \tag{14}$$

This system of equations is sufficient to calculate the flow-field properties, once appropriate expressions for the reaction-rate constants k_f and k_r have been determined. Matthews (ref. 7) gives the measured dissociation-rate constant for oxygen as

$$(k_f)_{meas} = (1.1 \times 10^{25})T^{-2.5} \exp\left(-\frac{59\,380}{T}\right) \frac{cm^3}{mole\text{-}sec} \tag{15}$$

Although the temperature range for the experiments of Matthews was 3000° K to 5000° K, equation (15) is used for much higher temperatures in the present applications. When the vibrational energy is in equilibrium with the translational mode, the forward and reverse rate constants are related through the equilibrium constant

$$K_e = \frac{(k_f)_{vib\ eq}}{k_r} \tag{16}$$

Since recombination for the flow over a wedge is negligible until the vibrational energy is close to equilibrium, the effect of vibrational nonequilibrium on k_r is neglected. The equilibrium constant for the dissociation of oxygen reaction is (ref. 12)

$$K_e = \frac{4m}{(h^3)}\frac{(\pi m k_B T)^{3/2}}{W}\frac{\Theta_R}{T}\left(1 - e^{-\Theta_v/T}\right)\frac{Q_O^2}{Q_{O_2}}e^{-\Theta_d/T}$$

where $\Theta_R = 2.059^\circ$ K. As indicated in appendix B of reference 14, the electronic partition functions for oxygen vary less than 5 percent for 1500° K < T < 8000° K. Therefore, average values over this temperature range are $Q_{O_2} = 3.3$ and $Q_O = 8.8$. The coupling effect of vibrational nonequilibrium on dissociation for the CVD and CVDV models is given by reference 1 as

$$f(T,T_v) \equiv \frac{k_f}{(k_f)_{vib\ eq}} = \frac{1}{N}\left[\frac{1 - \exp(-N\Theta_v/T_m)}{\exp(\Theta_v/T_m) - 1}\right]\left[\frac{\exp(\Theta_v/T_v) - 1}{\exp(\Theta_v/T) - 1}\right] \tag{17}$$

Equations (15), (16), and (17) can be used to compute k_f and k_r, provided a relationship between k_f and $(k_f)_{meas}$ or $(k_f)_{vib\ eq}$ and $(k_f)_{meas}$ is known. A survey of the literature indicates that several investigations (such as refs. 15 to 17) assumed the dissociation-rate constant for oxygen was measured with the vibrational energy in equilibrium. In his shock-tube experiments with oxygen, Matthews (ref. 7) observed a small relaxation region aft of the shock wave, but upstream of the reaction region. He therefore associated this small relaxation region with the vibrational relaxation and concluded that the vibrational energy was in equilibrium in the reaction zone where the experimental values of the dissociation-rate constants were obtained. However, in a more recent report Treanor (ref. 10) explains this phenomenon very differently. Treanor indicates that aft of the shock wave the vibrational temperature rises rapidly from room temperature then levels off at some higher temperature which is appreciably less than the translational temperature. (See fig. 2.) It is in this "quasi-equilibrium" zone (where T_v has leveled off) that the experimental values of dissociation-rate constants have been measured. Although $T_v < T$ in the quasi-equilibrium zone, the magnitudes of the first two terms on the right-hand side of equation (9) are nearly equal and the third term (recombination) is negligible, hence $\frac{dE_v}{dt} \approx 0$. Physically, the rate of increase of vibrational energy due to collisions is balanced by the loss of vibrational energy due to dissociation. Treanor further says, "thus during the entire time when the dissociation rate is being measured, the vibrational mode is out of equilibrium with the translational temperature, and the coupling of vibration and dissociation causes the observed rate to be less than the rate that would be obtained with local vibrational equilibrium." Although the quasi-equilibrium zone depicted in figure 2 is for 0.5 percent O_2 in 99.5 percent Ar, the normal shock computations in reference 2 indicate a similar quasi-equilibrium zone exists for undiluted O_2, which Matthews used in his experiments (ref. 7).

In reference 10 Treanor also gives an iterative method to obtain $(k_f)_{vib\ eq}$ from $(k_f)_{meas}$. However, it is cumbersome to apply this technique to two-dimensional flow-field computations since it would require iterations at every mesh point. To illustrate the possible deviations in the flow-field properties for the nonequilibrium flow of oxygen over a wedge (using the CVD and CVDV couplings), two interpretations of measured

dissociation-rate constants are considered. The first interpretation assumes

$$(k_f)_{meas} = (k_f)_{vib\ eq}$$

which is the assumption made in references 15 to 17. The other interpretation assumes that the measured rate constant already contains the vibrational nonequilibrium effects and thus sets

$$(k_f)_{meas} = k_f$$

It is believed that the computed flow properties for the CVD and CVDV coupling models using any other method of obtaining k_f from $(k_f)_{meas}$ should lie between these two limiting conditions.

Method for Numerical Computations

Let the flow field be divided into an orthogonal mesh system as shown in the following sketch:

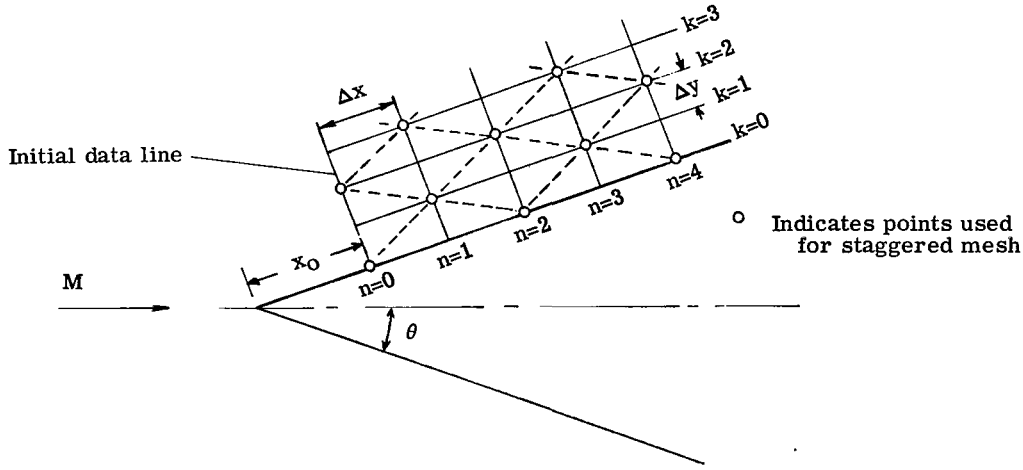

Then the coordinates of a general mesh point n,k are $x = x_0 + n\,\Delta x$ and $y = k\,\Delta y$. Approximate flow properties are first determined along the initial data line (n = 0) by using the exact wedge-tip gradients given in appendix C of reference 13. The numerical technique for computing the flow-field solution at increasing values of n is to replace the governing partial differential equations (eqs. (1) to (5)) with finite-difference equations.

The system of partial differential equations given by equations (1) to (5) may be written as the one vector equation:

$$\frac{\partial a_m}{\partial x} + \frac{\partial b_m}{\partial y} + d_m = 0 \qquad (m = 1, 2, 3, 4, 5) \qquad (18)$$

The difference scheme, suggested by Lax (ref. 18), replaces the partial derivative $\left(\frac{\partial a_m}{\partial x}\right)_{n,k}$ at the mesh point n,k with the modified forward difference quotient

$$\frac{(a_m)_{n+1,k} - \frac{1}{2}\left[(a_m)_{n,k+1} + (a_m)_{n,k-1}\right]}{\Delta x}$$

and replaces $\left(\frac{\partial b_m}{\partial y}\right)_{n,k}$ with the symmetric difference quotient

$$\frac{(b_m)_{n,k+1} - (b_m)_{n,k-1}}{2\,\Delta y}$$

Since only the mesh points $n,k+1$ and $n,k-1$ are involved at n for both of these difference quotients, the term $(d_m)_{n,k}$ is replaced by the average value

$$\frac{1}{2}\left[(d_m)_{n,k+1} + (d_m)_{n,k-1}\right]$$

With these substitutions the system of partial differential equations given by equation (18) is replaced with

$$(a_m)_{n+1,k} = \frac{1}{2}\left[(a_m)_{n,k+1} + (a_m)_{n,k-1}\right] - \frac{\Delta x}{2\,\Delta y}\left[(b_m)_{n,k+1} - (b_m)_{n,k-1}\right] - \frac{\Delta x}{2}\left[(d_m)_{n,k+1} + (d_m)_{n,k-1}\right] \qquad (m = 1, 2, 3, 4, 5) \qquad (19)$$

In this manner the flow-field properties at $n+1,k$ may be determined from those at $n,k+1$ and $n,k-1$. Therefore, starting with the approximate flow properties along the initial data line ($n = 0$), the flow properties can be calculated at all points of the staggered mesh $n = 1, 2, 3, \ldots$ and $k = 1, 3, 5, 7, \ldots$ when n is odd; and $k = 0, 2, 4, 6, \ldots$ when n is even. (See the sketch.)

Equation (19) cannot be used to compute the properties on the wedge surface ($k = 0$) unless imaginary properties are known at $k = -1$, which lies inside the wedge. It was found in reference 13 that the following difference scheme gave more accurate results along the surface than determining imaginary properties at $k = -1$ by an extrapolation or reflection technique and by using equation (19). Therefore, the finite-difference scheme for body points makes the following replacements:

$$\left(\frac{\partial a_m}{\partial x}\right)_{n,0} \rightarrow \frac{(a_m)_{n+1,0} - (a_m)_{n-1,0}}{2\,\Delta x}$$

$$\left(\frac{\partial b_m}{\partial y}\right)_{n,0} \rightarrow \frac{(b_m)_{n,1} - \frac{1}{2}\left[(b_m)_{n+1,0} + (b_m)_{n-1,0}\right]}{\Delta y}$$

$$(d_m)_{n,0} \rightarrow \frac{1}{2}\left[(d_m)_{n+1,0} + (d_m)_{n-1,0}\right]$$

Then the system of partial differential equations given by equation (18) becomes

$$(a_m + \Delta x\, d_m)_{n+1,0} = (a_m - \Delta x\, d_m)_{n-1,0} - \frac{2\,\Delta x}{\Delta y}\left[(b_m)_{n,1} - \frac{(b_m)_{n+1,0} + (b_m)_{n-1,0}}{2}\right] \qquad (20)$$

This equation can be simplified by noting that $(b_m)_{n+1,0} = (b_m)_{n-1,0} = 0$ for $m = 1, 2, 4$, and 5; and the $m = 3$ vector is not required on the surface because the boundary condition requires $v = 0$ at $k = 0$. Thus, the difference equation for the body points finally becomes

$$(a_m + \Delta x\, d_m)_{n+1,0} = (a_m - \Delta x\, d_m)_{n-1,0} - \frac{2\,\Delta x}{\Delta y}(b_m)_{n,1} \qquad (m = 1, 2, 4, 5) \qquad (21)$$

As a consequence of Lax's difference scheme an artificial viscosity is implicitly introduced and allows the computations to proceed downstream of the initial data line as if no shock wave were present at all. The shock wave appears in the solution, however, smeared over several mesh spaces while accurately giving the proper jump conditions across the shock. For more details concerning the numerical technique, consult reference 13.

Since the system of equations being solved is hyperbolic, the ratio of the mesh spacing in the x-direction to the mesh spacing in the y-direction is limited by the hyperbolic stability criterion. The free stream as well as the shock layer must be considered in determining the stability criterion because the computations carry through the shock wave. For all the examples given here, the free-stream stability criterion was more stringent than that of the shock layer since the free-stream velocity is inclined at the wedge half-angle θ to the coordinate system.

RESULTS AND DISCUSSION

It is well known that for the supersonic, inviscid flow of a frozen gas past a wedge, the attached shock wave is straight and the fluid properties are constant between the body surface and the wave. The same qualitative results also hold for a gas in equilibrium; however, in this case, the shock wave is closer to the body and the constant fluid properties are different from those of frozen flow. In particular, the equilibrium pressure and temperature are less than the corresponding properties for frozen flow.

When the conditions are such that nonequilibrium effects must be considered, the flow field is complicated. At the tip of the wedge the flow is frozen since it has just passed through the infinitesimally thin shock wave and has not had time to relax. The translational and rotational energy modes reach equilibrium almost immediately;

however, the vibrational and dissociational energies require a finite time to reach equilibrium. For an undissociated free stream, the vibrational energy and the degree of dissociation increase along the surface of the wedge. These conditions in turn decrease the temperature and pressure but increase the velocity and density. The shock wave is inclined at the angle for frozen flow at the tip, but bends downward and approaches the equilibrium angle far downstream. As the flow along the surface achieves an equilibrium condition downstream, the pressure is the same as that for the equilibrium wedge solution; however, the same is not true for the other flow variables. Downstream of the nose, three regions are observed in the profiles of properties between the body and the shock wave. Near the surface there exists an entropy layer since the streamlines passed through the steeper shock wave near the tip of the wedge. In the vicinity of the wave, the flow properties are close to being frozen since they have just passed through the shock wave and have not had time to relax. Between these two regions is a region which is essentially in equilibrium. This portion of the flow field has passed through the shock wave further upstream and thus has had time to relax to the equilibrium conditions.

The cases given below were computed to determine the differences between the two limiting conditions of $(k_f)_{meas} = (k_f)_{vib\ eq}$ and $(k_f)_{meas} = k_f$ for the nonequilibrium flow of oxygen over a wedge. In each case the shock-wave angle at the tip of the wedge was chosen to be 59^o, which is close to the shock detachment angle for the Mach numbers considered. The free-stream properties were chosen so that the shock strengths at the wedge tip would be the same as those for the normal shock solutions computed in reference 2 for oxygen.

Case I:

$$M = 9.45099 \qquad \theta = 42.379^o$$

Case II:

$$M = 27.17159 \qquad \theta = 43.361^o$$

For each case,

$$T_\infty = 249^o\ K \qquad p_\infty = 2.23 \times 10^{-4}\ atm$$

$$E_{v,\infty} = 0 \qquad \alpha_\infty = 0$$

Figures 3 and 4 show the variation of $\overline{T}$, $\overline{E}_v$, and α along the wedge surface for case I. Figure 4 illustrates the lag in the dissociational rate for $(k_f)_{meas} = (k_f)_{vib\ eq}$ as compared with $(k_f)_{meas} = k_f$ along the wedge surface. However, since the degree of dissociation is small, there is very little difference between the two limiting conditions for the variation of $\overline{T}$ and $\overline{E}_v$ along the surface. Also, there is no noticeable

difference between the CVD and CVDV models for this case. Although $\overline{T}$ and $\overline{E}_v$ are close to equilibrium at $x = 80$ cm, α is still increasing and additional computations showed that α had not achieved an equilibrium condition as far downstream as $x = 4750$ cm.

The variation of $\overline{T}$, $\overline{E}_v$, and α along the wedge surface for case II is shown in figures 5, 6, and 7, respectively. For this case there are significant differences between the two limiting conditions as well as between the CVD and CVDV models. Figure 6 shows that the vibrational energy for the CVDV models levels off for $2 \text{ cm} \lessapprox x \lessapprox 20 \text{ cm}$ and then increases to an equilibrium value near $x = 100$ cm. This zone is similar to the quasi-equilibrium region noted in figure 2 for the flow aft of a shock wave. Figure 7 also depicts a lag in the dissociation rate near the tip of the wedge for $(k_f)_{meas} = (k_f)_{vib\ eq}$ as was found in case I. Figures 8, 9, and 10 show the profiles of $\overline{T}$, $\overline{E}_v$, and α normal to the wedge surface at $x = 3$ cm. These figures illustrate that the shock-layer thickness is largest for the $(k_f)_{meas} = (k_f)_{vib\ eq}$ condition with the CVDV model.

The condition $(k_f)_{meas} = k_f$ for the CVD model was found to yield the same results as computations with no coupling between the vibrations and dissociation ($f \equiv 1$). This unusual circumstance is attributed to the fact that the coupling factor f given by equation (17) only affects k_r (for the $(k_f)_{meas} = k_f$ condition), and for the flow over a wedge recombination is only significant in the regions where the vibrational energy is near equilibrium (hence $f \approx 1$).

CONCLUDING REMARKS

To illustrate two different interpretations of measured dissociation-rate constants, the nonequilibrium flow of oxygen over a wedge was computed with the CVD and CVDV coupling models for the two limiting conditions $(k_f)_{meas} = (k_f)_{vib\ eq}$ and $(k_f)_{meas} = k_f$ (where k_f is forward reaction-rate constant and the subscripts meas and vib eq refer to measured and vibrational equilibrium, respectively). These limiting conditions should provide bounds for flow properties computed using any other method of obtaining k_f from $(k_f)_{meas}$ with the previously mentioned coupling models.

For the lower Mach numbers, where dissociation is small, there is very little difference between the flow properties for the two limiting conditions, with the exception of the atom mass fraction. There is a noticeable lag of α (atom mass fraction) with $(k_f)_{meas} = (k_f)_{vib\ eq}$ behind α with $(k_f)_{meas} = k_f$; however, since the degree of dissociation is small, these effects are insignificant as far as the other flow-field properties are concerned.

At the higher Mach numbers, where dissociation is significant, appreciable differences are found between the two limiting conditions for all the flow-field properties.

Until a better understanding of the measured reaction rates is obtained, calculations should be made for the two limiting conditions to indicate the possible range in magnitude of the flow variables.

Langley Research Center,
National Aeronautics and Space Administration,
Langley Station, Hampton, Va., December 20, 1966,
129-01-08-18-23.

REFERENCES

1. Hammerling, P.; Teare, J. D.; and Kivel, B.: Theory of Radiation From Luminous Shock Waves in Nitrogen. Phys. Fluids, vol. 2, no. 4, July-Aug. 1959, pp. 422-426.

2. Treanor, Charles E.; and Marrone, Paul V.: Effect of Dissociation on the Rate of Vibrational Relaxation. Phys. Fluids, vol. 5, no. 9, Sept. 1962, pp. 1022-1026.

3. DeJarnette, Fred R.: Effects of Two Vibration-Dissociation Coupling Models on Nonequilibrium Hypersonic Flow of Nitrogen Over a Wedge. NASA TN D-3521, 1966.

4. Marrone, Paul V.; and Treanor, Charles E.: Chemical Relaxation With Preferential Dissociation From Excited Vibrational Levels. Phys. Fluids, vol. 6, no. 9, Sept. 1963, pp. 1215-1221.

5. Treanor, C. E.: Coupling of Vibration and Dissociation in Gasdynamic Flows. Paper No. 65-29, Am. Inst. Aeron. Astronaut., Jan. 1965.

6. Tirumalesa, Duvvuri: Nozzle Flows With Coupled Vibration and Dissociational Nonequilibrium. Paper No. 66-520, Am. Inst. Aeron. Astronaut., June 1966.

7. Matthews, D. L.: Interferometric Measurement in the Shock Tube of the Dissociation Rate of Oxygen. Phys. Fluids, vol. 2, no. 2, Mar.-Apr. 1959, pp. 170-178.

8. Byron, Stanley R.: Measurement of the Rate of Dissociation of Oxygen. J. Chem. Phys., vol. 30, no. 6, June 1959, pp. 1380-1392.

9. Camac, Morton; and Vaughan, Arthur: O_2 Dissociation Rates in O_2-Ar Mixtures. J. Chem. Phys., vol. 34, no. 2, Feb. 1961, pp. 460-470.

10. Treanor, Charles E.: Vibrational Relaxation Effects in Dissociation Rate-Constant Measurements. Rept. No. AG-1729-A-1 (Contract No. NASr-119), Cornell Aeron. Lab., Inc., Aug. 1962.

11. Wray, Kurt L.: Shock-Tube Study of the Coupling of the O_2-Ar Rates of Dissociation and Vibrational Relaxation. J. Chem. Phys., vol. 37, no. 6, Sept. 15, 1962, pp. 1254-1263.

12. Vincenti, Walter G.; and Kruger, Charles H., Jr.: Introduction to Physical Gas Dynamics. John Wiley and Sons, Inc., c.1965.

13. DeJarnette, Fred R.: Application of Lax's Finite Difference Method to Nonequilibrium Hypersonic Flow Problems. NASA TR R-234, 1966.

14. Heims, Steve P.: Effects of Chemical Dissociation and Molecular Vibrations on Steady One-Dimensional Flow. NASA TN D-87, 1959.

15. Wray, Kurt L.; and Teare, J. Derek: Shock-Tube Study of the Kinetics of Nitric Oxide at High Temperatures. J. Chem. Phys., vol. 36, no. 10, May 15, 1962, pp. 2582-2596.

16. Marrone, Paul V.: Inviscid, Nonequilibrium Flow Behind Bow and Normal Shock Waves, Part I. General Analysis and Numerical Examples. Rept. No. QM-1626-A-12(I) (Contract No. DA-30-069-ORD-3443), Cornell Aeron. Lab., Inc., May 1963.

17. Greenblatt, M.: The Coupling of Vibrational Relaxation and Dissociation. VKI-TN-19, Von Karman Inst. Fluid Dyn., 1964.

18. Lax, Peter D.: Weak Solutions of Nonlinear Hyperbolic Equations and Their Numerical Computation. Commun. Pure Appl. Math., vol. VII, no. 1, Feb. 1954, pp. 159-193.

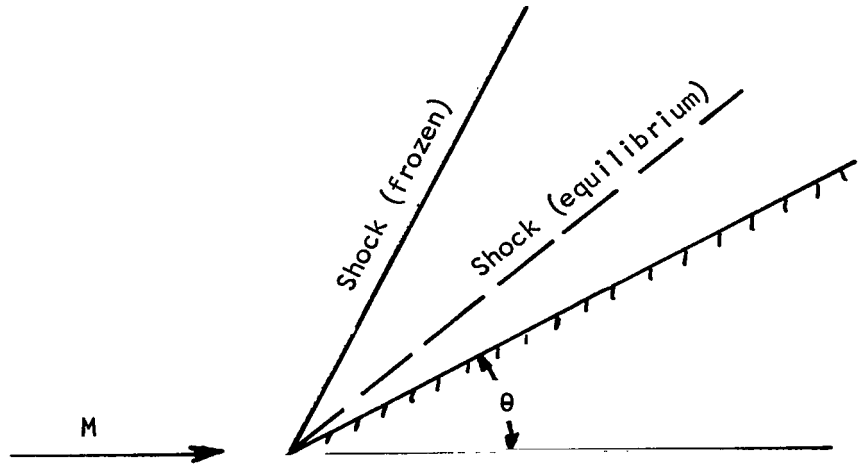

(a) Frozen and equilibrium.

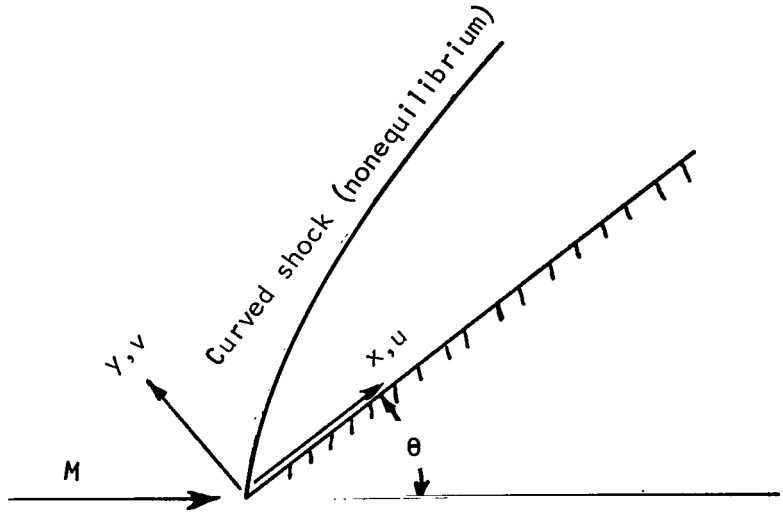

(b) Nonequilibrium.

Figure 1.- Flow past a wedge.

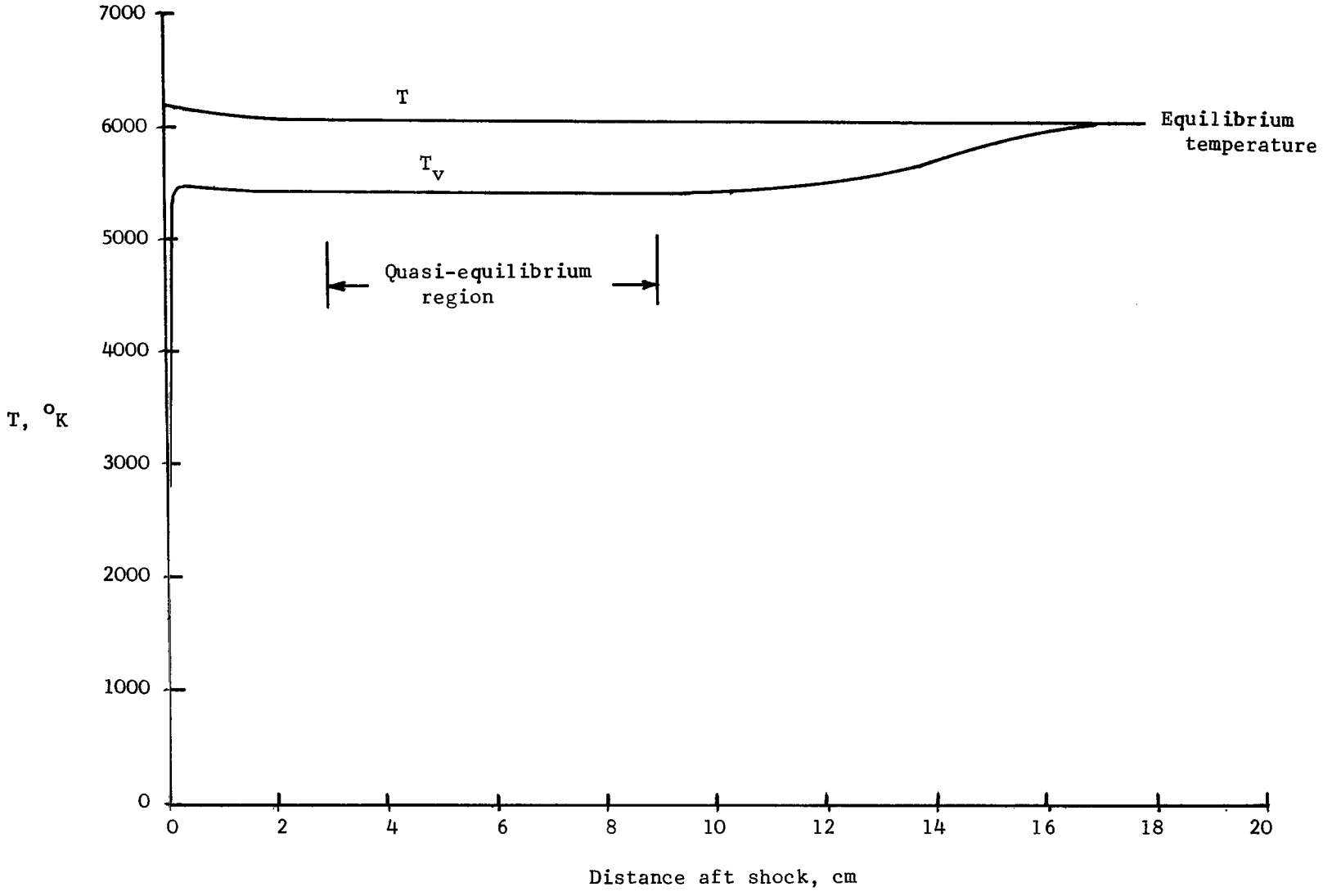

Figure 2.- Temperature behind normal shock (from ref. 10). $P_\infty = 1.33 \times 10^{-2}$ atm; $V_\infty = 2.56 \times 10^5$ cm/sec; gas: 99.5% Ar, 0.5% O_2.

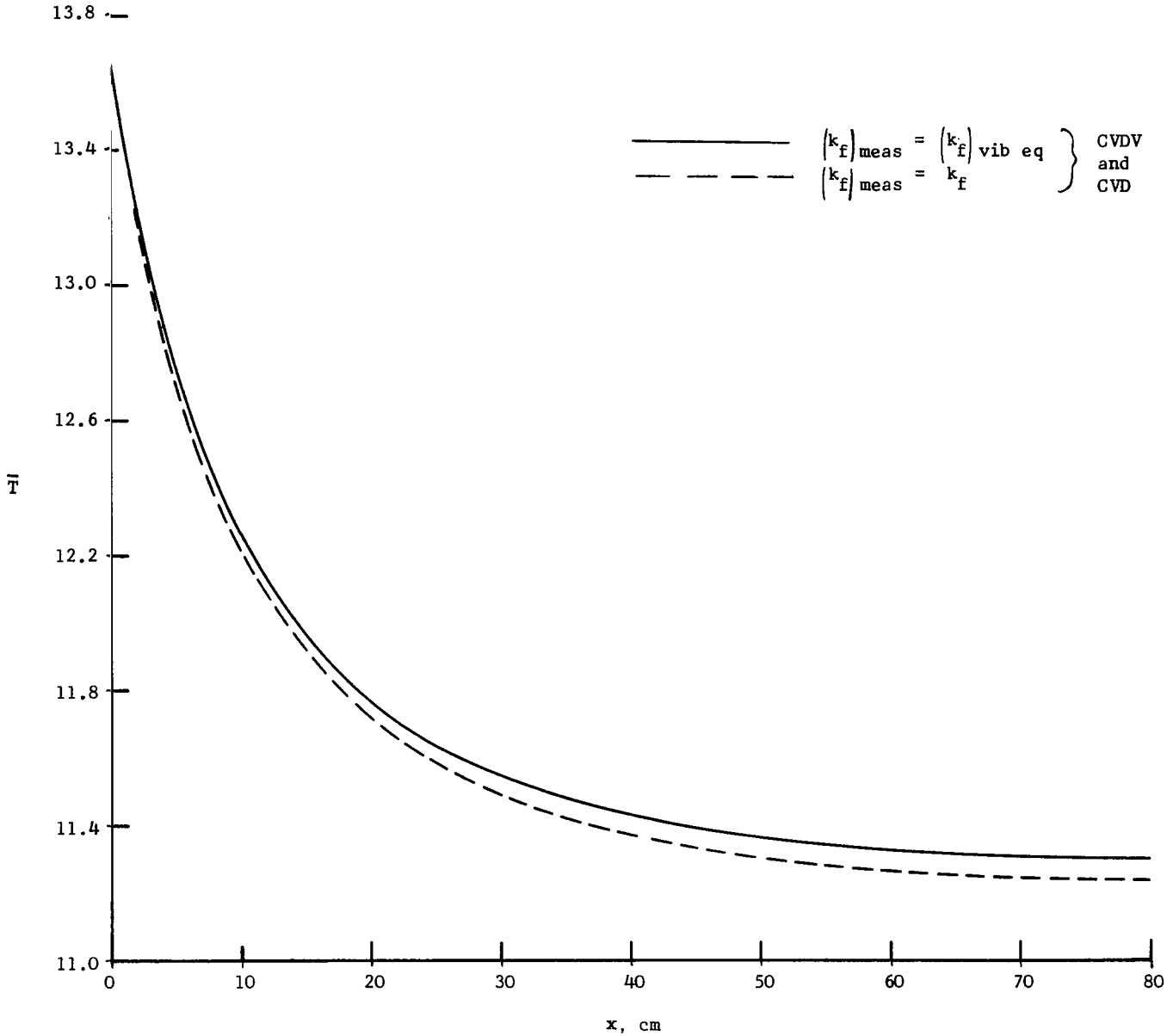

Figure 3.- Temperature along wedge surface for case I. M = 9.45; $\theta = 42.38^0$.

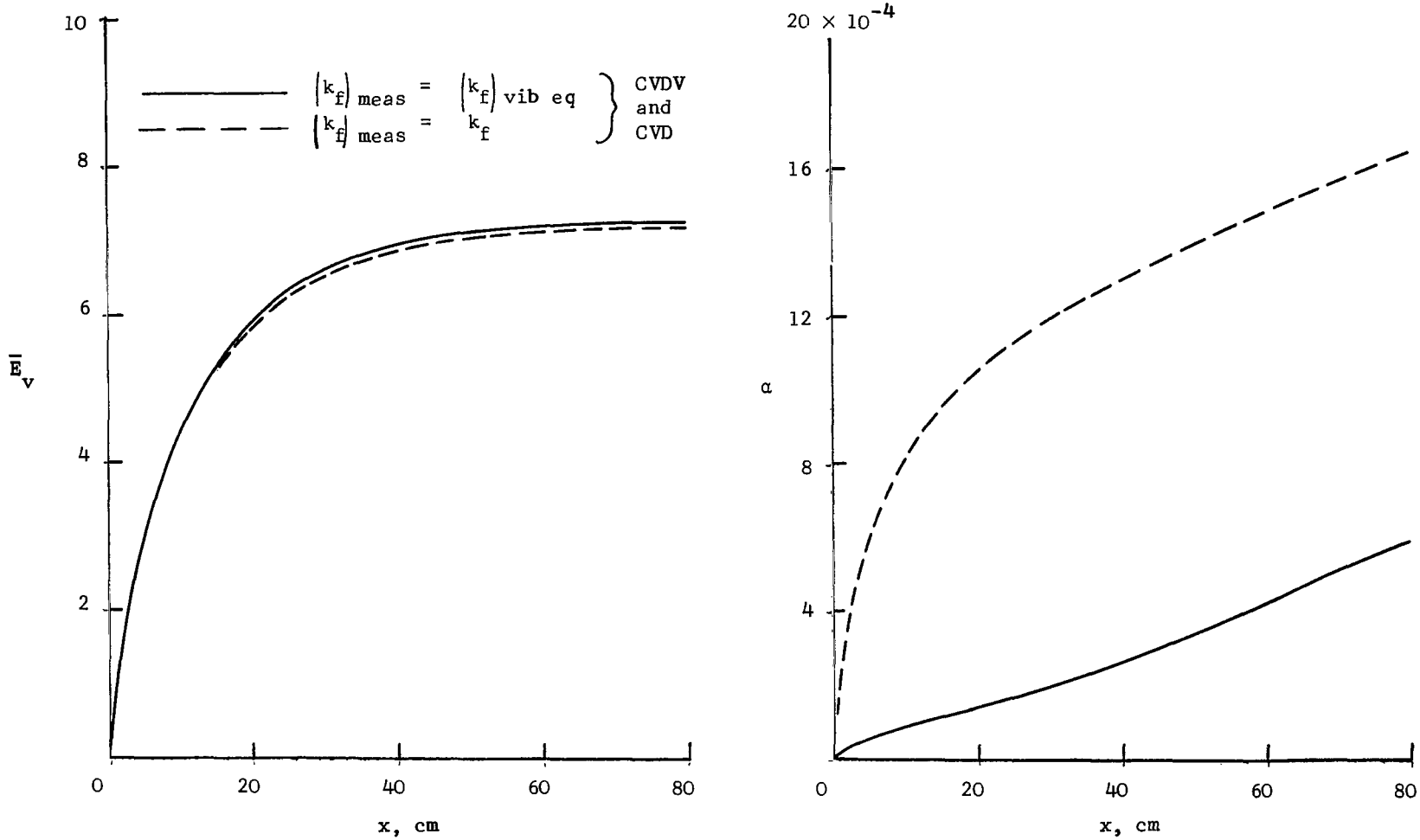

Figure 4.- Vibrational energy and atom mass fraction along wedge surface for case I. M = 9.45; $\theta = 42.38^0$.

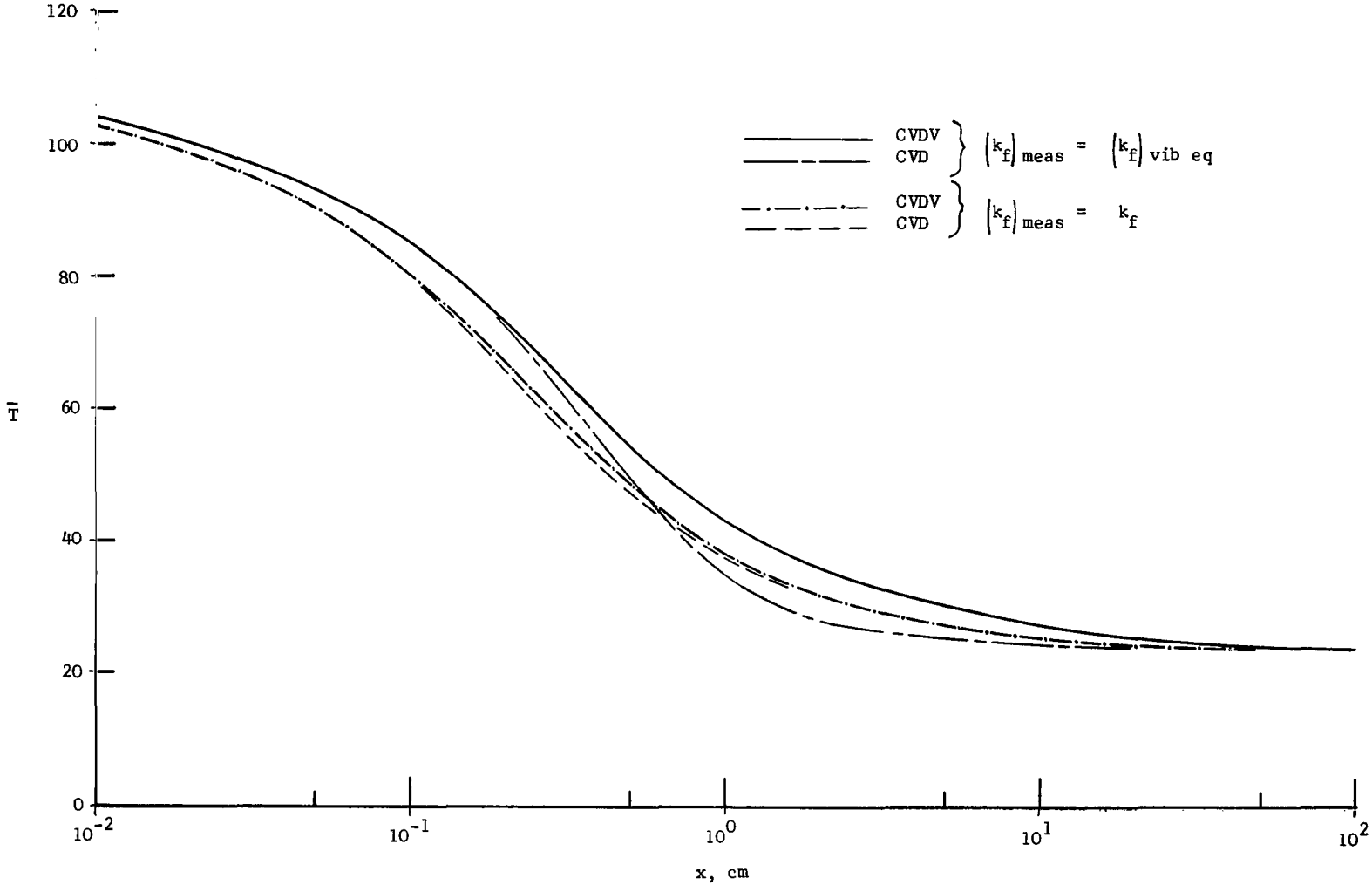

Figure 5.- Temperature along wedge surface for case II. M = 27.17; $\theta = 43.36^{0}$.

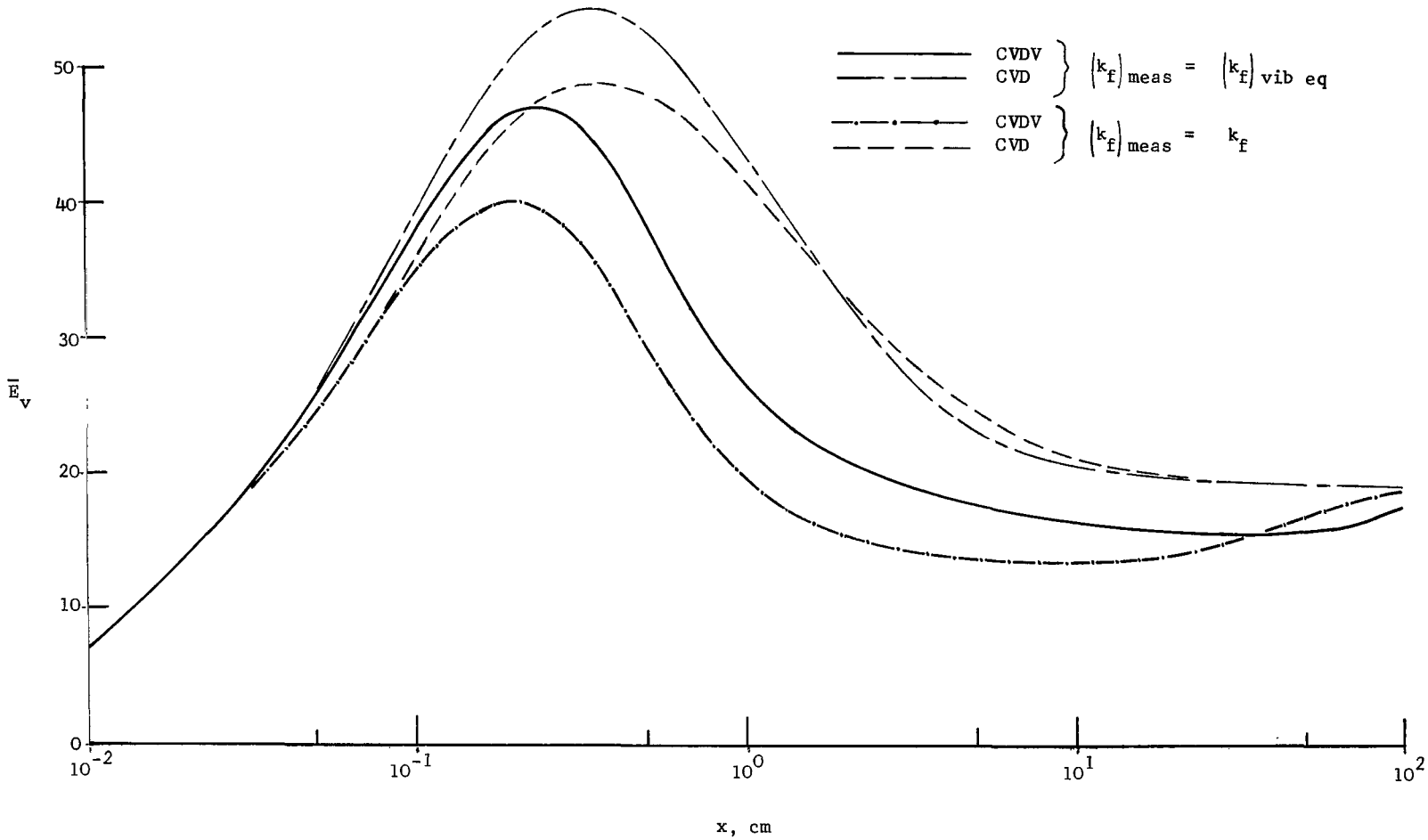

Figure 6.- Vibrational energy along wedge surface for case II. M = 27.17; $\theta = 43.36^0$.

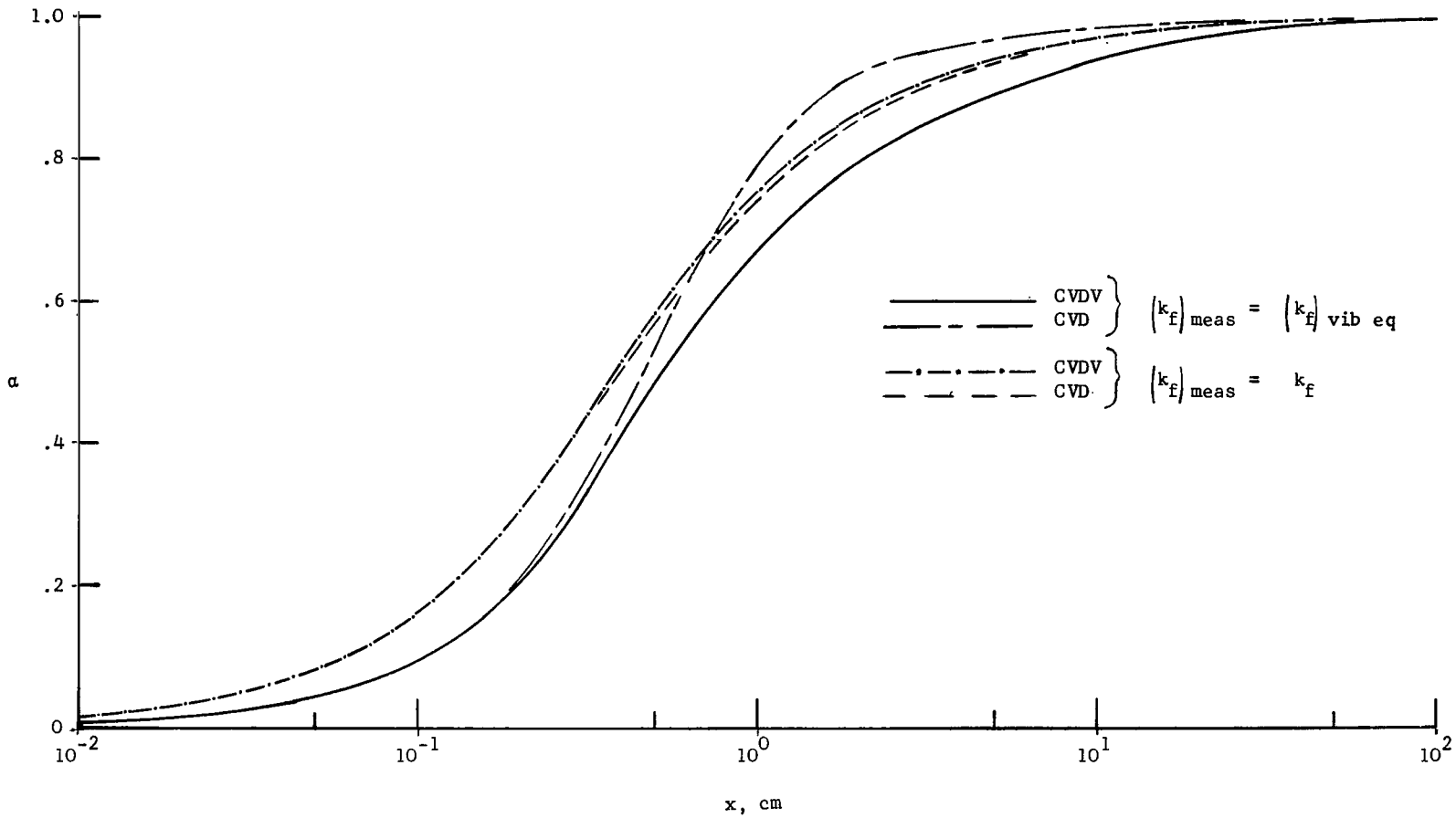

Figure 7.- Atom mass fraction along wedge surface for case II. M = 27.17; $\theta = 43.36^0$.

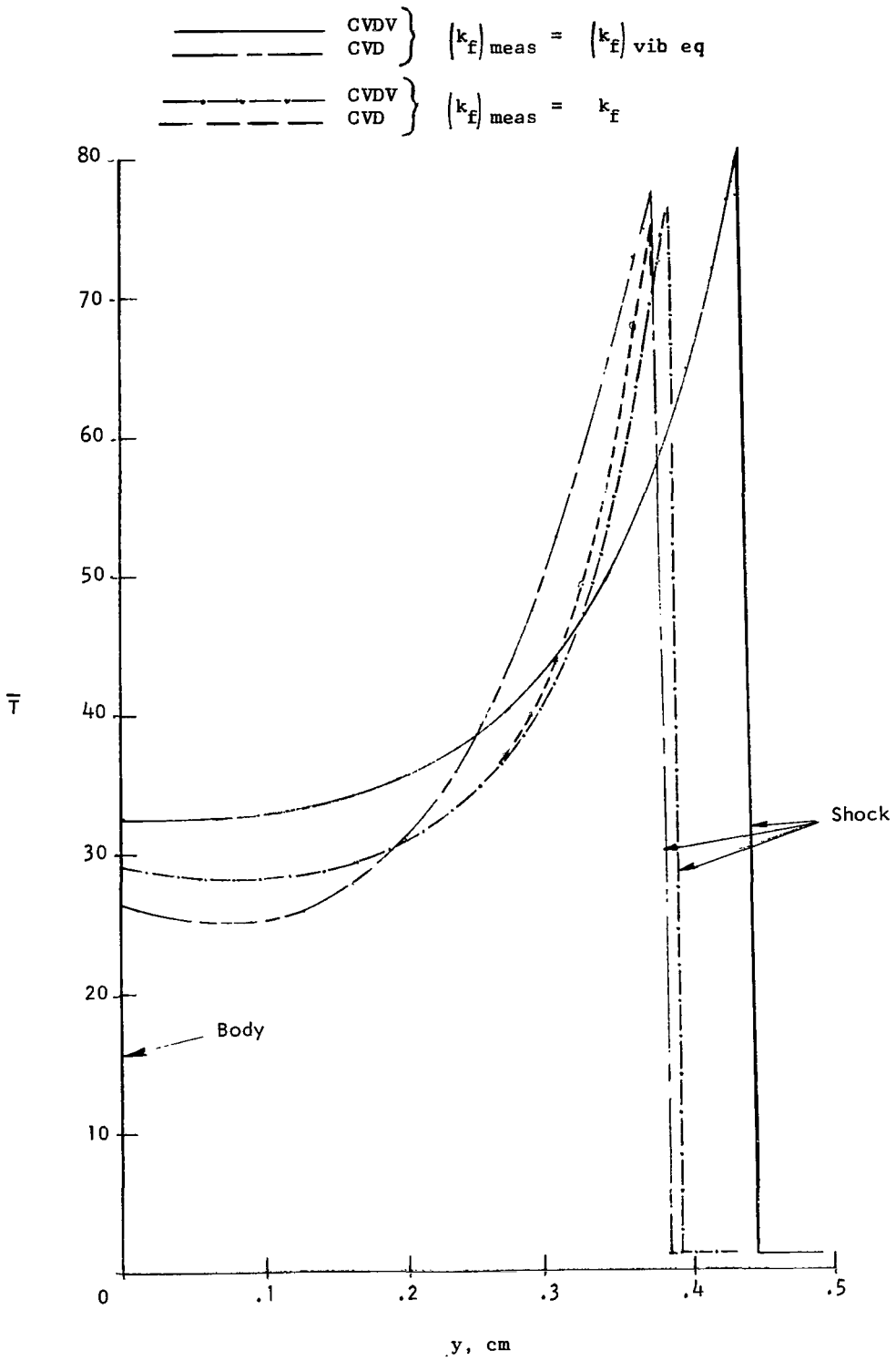

Figure 8.- Temperature profile normal to wedge surface at x = 3 cm for case II. M = 27.17; $\theta = 43.36^0$.

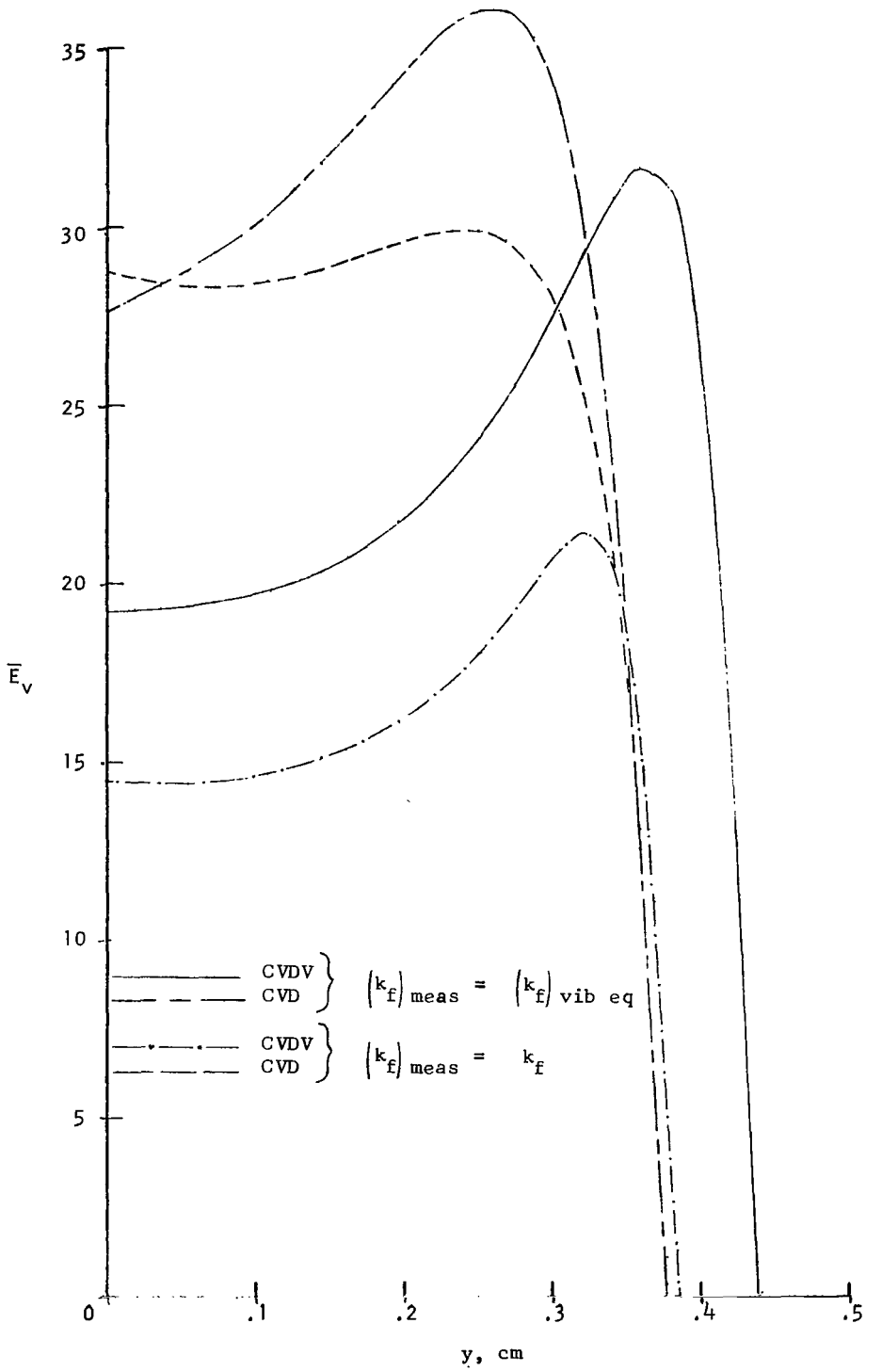

Figure 9.- Vibrational energy profile normal to wedge surface at x = 3 cm for case II. M = 27.17; $\theta = 43.36^0$.

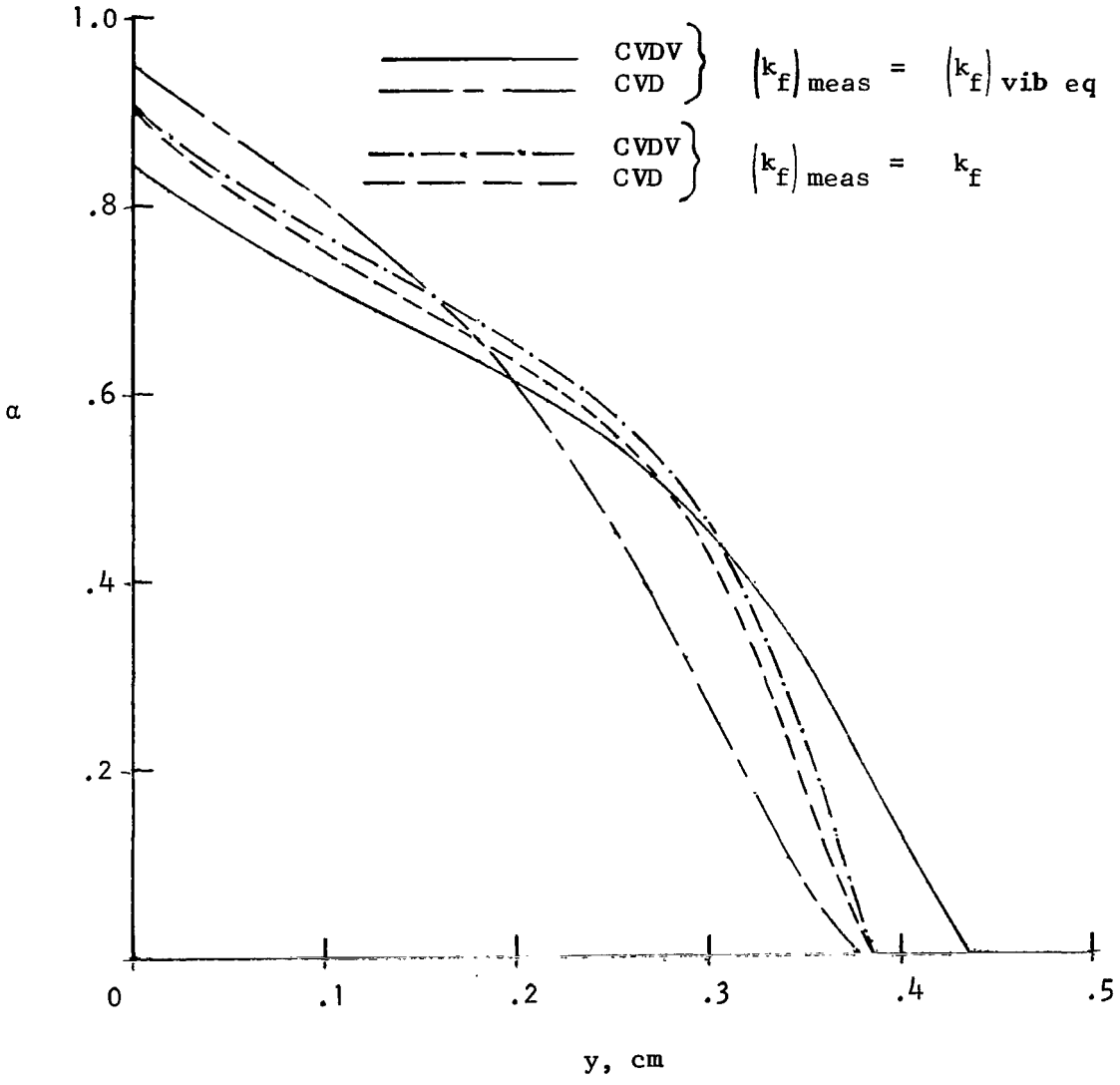

Figure 10.- Atom mass fraction profile normal to wedge surface at x = 3 cm for case II. M = 27.17; $\theta = 43.36^0$.

NASA-Langley, 1967 —— 12 L-5269

"The aeronautical and space activities of the United States shall be conducted so as to contribute . . . to the expansion of human knowledge of phenomena in the atmosphere and space. The Administration shall provide for the widest practicable and appropriate dissemination of information concerning its activities and the results thereof."

—NATIONAL AERONAUTICS AND SPACE ACT OF 1958

NASA SCIENTIFIC AND TECHNICAL PUBLICATIONS

TECHNICAL REPORTS: Scientific and technical information considered important, complete, and a lasting contribution to existing knowledge.

TECHNICAL NOTES: Information less broad in scope but nevertheless of importance as a contribution to existing knowledge.

TECHNICAL MEMORANDUMS: Information receiving limited distribution because of preliminary data, security classification, or other reasons.

CONTRACTOR REPORTS: Scientific and technical information generated under a NASA contract or grant and considered an important contribution to existing knowledge.

TECHNICAL TRANSLATIONS: Information published in a foreign language considered to merit NASA distribution in English.

SPECIAL PUBLICATIONS: Information derived from or of value to NASA activities. Publications include conference proceedings, monographs, data compilations, handbooks, sourcebooks, and special bibliographies.

TECHNOLOGY UTILIZATION PUBLICATIONS: Information on technology used by NASA that may be of particular interest in commercial and other non-aerospace applications. Publications include Tech Briefs, Technology Utilization Reports and Notes, and Technology Surveys.

Details on the availability of these publications may be obtained from:

SCIENTIFIC AND TECHNICAL INFORMATION DIVISION

NATIONAL AERONAUTICS AND SPACE ADMINISTRATION

Washington, D.C. 20546